Received: 22 June 2023 | Revised: 21 September 2023 | Accepted: 1 October 2023

DOI: 10.1111/exd.14952

Experimental Dermatology WILEY

RESEARCH ARTICLE

Lesional skin of seborrheic dermatitis patients is characterized by skin barrier dysfunction and correlating alterations in the stratum corneum ceramide composition

Jannik Rousel[1,2] | Andreea Nădăban[2] | Mahdi Saghari[1,3] | Lisa Pagan[1,3] | Ahnjili Zhuparris[1,3,4] | Bart Theelen[5] | Tom Gambrah[1] | Hein E. C. van der Wall[1] | Rob J. Vreeken[6] | Gary L. Feiss[7] | Tessa Niemeyer-van der Kolk[1] | Jacobus Burggraaf[1,2,3] | Martijn B. A. van Doorn[1,8] | Joke A. Bouwstra[2] | Robert Rissmann[1,2,3]

[1]Centre for Human Drug Research, Leiden, The Netherlands

[2]Leiden Academic Centre for Drug Research, Leiden University, Leiden, The Netherlands

[3]Leiden University Medical Center, Leiden, The Netherlands

[4]Leiden Institute of Advanced Computer Science, Leiden University, Leiden, Netherlands

[5]Westerdijk Fungal Biodiversity Institute, Utrecht, The Netherlands

[6]Maastricht Multimodal Molecular Imaging Institute, Maastricht University, Maastricht, The Netherlands

[7]Cutanea Life Sciences, Wayne, Pennsylvania, USA

[8]Department of Dermatology, Erasmus Medical Centre, Rotterdam, The Netherlands

Correspondence
Robert Rissmann, Centre for Human Drug Research, Zernikedreef 8, 2333CL Leiden, The Netherlands.
Email: rrissmann@chdr.nl

Funding information
Cutanea Life Sciences, Wayne, Pennsylvania, USA; Maruho Co. Ltd., Kyoto, Japan

Abstract

Seborrheic dermatitis (SD) is a chronic inflammatory skin disease characterized by erythematous papulosquamous lesions in sebum rich areas such as the face and scalp. Its pathogenesis appears multifactorial with a disbalanced immune system, *Malassezia* driven microbial involvement and skin barrier perturbations. Microbial involvement has been well described in SD, but skin barrier involvement remains to be properly elucidated. To determine whether barrier impairment is a critical factor of inflammation in SD alongside microbial dysbiosis, a cross-sectional study was performed in 37 patients with mild-to-moderate facial SD. Their lesional and non-lesional skin was comprehensively and non-invasively assessed with standardized 2D-photography, optical coherence tomography (OCT), microbial profiling including *Malassezia* species identification, functional skin barrier assessments and ceramide profiling. The presence of inflammation was established through significant increases in erythema, epidermal thickness, vascularization and superficial roughness in lesional skin compared to non-lesional skin. Lesional skin showed a perturbed skin barrier with an underlying skewed ceramide subclass composition, impaired chain elongation and increased chain unsaturation. Changes in ceramide composition correlated with barrier impairment indicating interdependency of the functional barrier and ceramide composition. Lesional skin showed significantly increased *Staphylococcus* and decreased *Cutibacterium* abundances but similar *Malassezia* abundances and mycobial composition compared to non-lesional skin. Principal component analysis highlighted barrier properties as main discriminating features. To conclude, SD is associated with skin barrier dysfunction and changes in the ceramide composition. No significant differences in the abundance of *Malassezia* were observed. Restoring the cutaneous barrier might be a valid therapeutic approach in the treatment of facial SD.

KEYWORDS
barrier, ceramides, *Malassezia*, seborrheic dermatitis, *staphylococcus*

1 | INTRODUCTION

Seborrheic dermatitis (SD) is an inflammatory, eczematous skin disease of the face and scalp with a multifactorial underlying pathophysiology. SD is characterized by the development of erythematous, scaly and itchy skin on seborrheic areas with high sebaceous gland activity such as the nasolabial folds, eyebrows and upper chest (Figure S1).[1] The exact pathophysiology of SD remains unclear due to its multifactorial and complex aetiology. Three major interdependent driving factors of the aberrant immunological responses behind SD are (I) individual susceptibility due to an imbalanced immune system leading to inflammation, (II) cutaneous microbial dysbiosis with pronounced colonization by *Malassezia* species and (III) a perturbed epidermal barrier.[1,2]

While these three hallmarks all contribute towards the development of SD, much emphasis has been on the microbiome and especially the involvement of *Malassezia*. *Malassezia* is a commensal yeast which is regarded as a key pathogen due to its concurrence with lesional skin and the clinical response of SD to antifungals.[3] It is hypothesised that the predilection of *Malassezia* for sebum-rich skin sites is due to its inability to perform de novo fatty acid synthesis, necessitating the processing of exogenous lipids which disturbs the epidermal barrier integrity and enables inflammation.[4,5] While this provides rationale for why inflammation is limited to these areas, it has been shown that neither the amount of *Malassezia*[5,6] nor an increased level of sebum production[1,2,6] are strictly tied to the development of SD.

Due to the implication that external triggers such as *Malassezia* and its metabolites can penetrate the skin,[7] the cutaneous barrier function itself has been proposed to be involved in SD pathogenesis.[6] The epidermal barrier function is located in the stratum corneum which consists of layers of cornified cells embedded in a lipid matrix mainly composed of cholesterol, fatty acids and ceramides.[8] Changes in the composition and consequently the lipid organization of this matrix directly impacts skin permeability.[9,10] Barrier perturbations and simultaneous alterations of the lipid matrix composition, such as reduced chain length and changes in ceramide subclass composition, have been observed in other inflammatory skin diseases such as atopic dermatitis and psoriasis.[11,12] This raised the question whether barrier repair can be exploited as a treatment option.[13]

The apparent contribution of host immunity, the microbiome and cutaneous barrier to the development of SD warrants a multimodal assessment for phenotyping SD. In this study, we established cutaneous inflammation by clinical scoring complemented with imaging. We elucidated the bacterial and fungal composition as both are implicated in SD,[14] with additional species-level profiling of *Malassezia*. Lastly, the cutaneous barrier function was characterized in-depth by trans-epidermal water loss (TEWL) measurements complemented with ceramide profiling using lipidomic analysis. This might yield new insights into how these modalities are implicated in disease.

2 | METHODS

An extended version of the methods can be found in the supporting information provided online.

2.1 | Study design and population

The study was conducted at the Centre for Human Drug Research (Leiden, the Netherlands) from November 2018 to January 2020 following the Declaration of Helsinki principles after approval by the medical ethics committee Stichting Beoordeling Ethiek Biomedisch Onderzoek (Assen, the Netherlands). Patients gave written informed consent prior to participation in the study. The use of SD medication was prohibited prior to enrolment for a period of 2 weeks for topical treatments, including dandruff shampoos, 3 weeks for phototherapy and 4 weeks for systemic treatments. In total, 37 patient exhibiting mild-to-moderate SD defined by an Investigator's Global Assessment (IGA) score of 2–3 after verification by a dermatologist were included and assessments performed during a single visit. Due to the heterogeneous presentation of SD and the invasiveness of assessments, assessments are performed on different sites of the face as listed in Table S1–S3. See Supplementary Material for further details.

2.2 | Clinical characteristics

Disease severity was scored using the Seborrheic Dermatitis and Severity Index (SDASI) adapted from Baysal, et al.,[15] 5-point IGA and percentage affected body surface area (%BSA). Patient reported outcomes included the 0–100 Numeric Rating Scale (NRS) itch, 5-Domain Itch Questionnaire[16] and Dermatology Life Quality Index (DLQI).[17,18] See Supplementary Material for further details.

2.3 | Standardized photography

Standardized two dimensional cross-polarized images of the face were taken using a VISIA-CR (Canfield Scientific). Erythema Index calculations were performed based on a method by Yamamoto, et al.[19] See Supplementary Material for further details.

2.4 | Optical coherence tomography

Lesional and non-lesional skin was imaged by Vivosight Dx optical coherence tomography (OCT) (Michelson Diagnostics, Kent) and epidermal thickness, superficial roughness and average epidermal vascularization were determined. See Supplementary Material for further details.

2.5 | Microbiome composition

Skin swabs were collected by rubbing the skin for 10 s. Swabs were extracted and 16 s rRNA and internal transcribed spacer (ITS) sequencing was performed to determine the bacterial and fungal composition, respectively. After genus level classification, microbes contributing <1% of the total were excluded and relative abundances determined. See Supplementary Material for further details.

2.6 | *Malassezia* culturing

Agar plates with modified Dixon medium were pressed against the skin for 20 s and cultured for *Malassezia*. *Malassezia* species determination by matrix-assisted laser desorption ionization-time of flight mass spectrometry (MALDI-TOF MS) was performed on mycological isolates as described by Kolecka et al.[20] See Supplementary Material for further details.

2.7 | Skin barrier integrity by trans-epidermal water loss

Subjects were allowed to acclimatize to controlled environmental conditions (humidity <60%, temperature 22 ± 2°C) in rested state for at least 15 min prior to measurements. TEWL was measured using an AquaFlux AF200 (Biox Systems Ltd.). See Supplementary Material for further details.

2.8 | Skin barrier lipidomics

Stratum corneum was harvested with four polyphenylene sulfide tape (Nichiban) after applying pressure using a D500 D-squame Pressure Instrument (CuDerm Corporation). Tapes were extracted and the ceramide fraction analysed through a validated liquid chromatography-mass spectrometry (LC–MS) setup as described by Boiten et al.[21] Figure S2 lists the 12 most prevalent ceramide classes included in the analysis using the nomenclature by Motta et al.[22] Sebum levels were determined using a Sebumeter SM815 (Courage+Khazaka, Köln, Germany). See Supplementary Material for further details.

2.9 | Statistical analysis

Data visualization and statistical testing were performed using Prism 9 (Graphpad Software). Two-way ANOVA, or a mixed effects model in the case of missing data points, was performed using Bonferroni's multiple comparison test in the case of multiple variables and paired t-test in the case of two variables. *p*-values are denoted as ns: $p > 0.05$, *: $p \leq 0.05$, **: $p \leq 0.01$, ***: $p \leq 0.001$. Integrative data graphing by principal component analysis (PCA) and min-max radar plotting has been performed through Python version 3.8.0 (Python Software Foundation). See Supplementary Material for further details.

TABLE 1 Baseline demographics including clinical scoring and patient reported outcomes from the study population. The minimal and maximal values are indicated among their respective scores.

Subjects (*n*)	37
Age (years)	37.8 ± 15.6
BMI (kg/m^2)	25.4 ± 3.4
Sex	
Female	5 (13.5%)
Male	32 (86.5%)
Race	
Asian	1 (2.7%)
Mixed (White, African)	1 (2.7%)
Latino	1 (2.7%)
White	34 (91.9%)
Fitzpatrick skin type	
1	4 (10.8%)
2	19 (51.4%)
3	13 (35.1%)
4	1 (2.7%)
5	0 (0.0%)
6	0 (0.0%)
Seborrheic Dermatitis Area and Severity index (0–45) (Mean ± SD)	7.0 ± 4.3
Investigator's Global Assessment	
1 (almost clear)	4 (10.8%)
2 (mild)	19 (51.4%)
3 (moderate)	13 (35.1%)
4 (severe)	1 (2.7%)
Affected body surface area (%) (Mean ± SD)	1.3 ± 0.7
Dermatology Life Quality Index (0–30) (Mean ± SD)	7.2 ± 5.5
Average Itch Numeric Rating scale (0–100) (Mean ± SD)	23.6 ± 22.5
5-Domain Itch Scale (5–25) (Mean ± SD)	11.6 ± 03.2

Abbreviations: BMI, body mass index; SD, standard deviation.

3 | RESULTS

In total, 37 patients were enrolled into the study. The patient population exhibited mild-to-moderate SD as shown by a SDASI score of 7.0 ± 4.3 and IGA score of ≤3 for 97% of all patients (Table 1). Patient reported disease burden was rated mild-to-moderate as evident from the DLQI (7.2 ± 5.5/30; 'moderate effect on patient's life'), average itch rating scale (23.6 ± 22.5/100) and 5-Domain itch scale rating (11.6 ± 3.2/25).

3.1 | Inflammation

Apart from clinical scoring, hallmarks of inflammation were assessed using standardized 2D-photography and OCT. Lesional skin had a significantly higher erythema index compared to non-lesional skin (67.62 AU vs. 49.19 AU, $p \leq 0.001$, Figure 1A). Despite high epidermal disorganization hampering the localization of the dermal-epidermal junction in multiple measurements, the epidermis of lesional skin was significantly thicker compared to non-lesional skin (0.15 mm vs. 0.10 mm, $p \leq 0.001$, Figure 1B). Superficial roughness of the skin was significantly increased in lesional skin (0.013 AU vs. 0.009 AU, $p \leq 0.001$, Figure 1C). Higher superficial vascularization was observed in lesional skin compared to non-lesional skin at a shallow skin depth of 0.1–0.25 mm ($p \leq 0.05$–0.001, Figure 1D) with no significant differences at greater depths. This culminates to an increased average vascularization between 0.1 and 0.25 mm of 0.079 in lesional skin compared to 0.058 in non-lesional skin ($p \leq 0.001$, Figure S3).

3.2 | Microbiome

After establishing the presence of inflammation, the facial microbial composition was investigated using 16 s rRNA and ITS sequencing for the bacterial and fungal microbiome, respectively. Neither Shannon indexes showed a significant difference between lesional and non-lesional skin sites (1.55 vs. 1.71, $p > 0.24$ and 0.58 vs. 0.66,

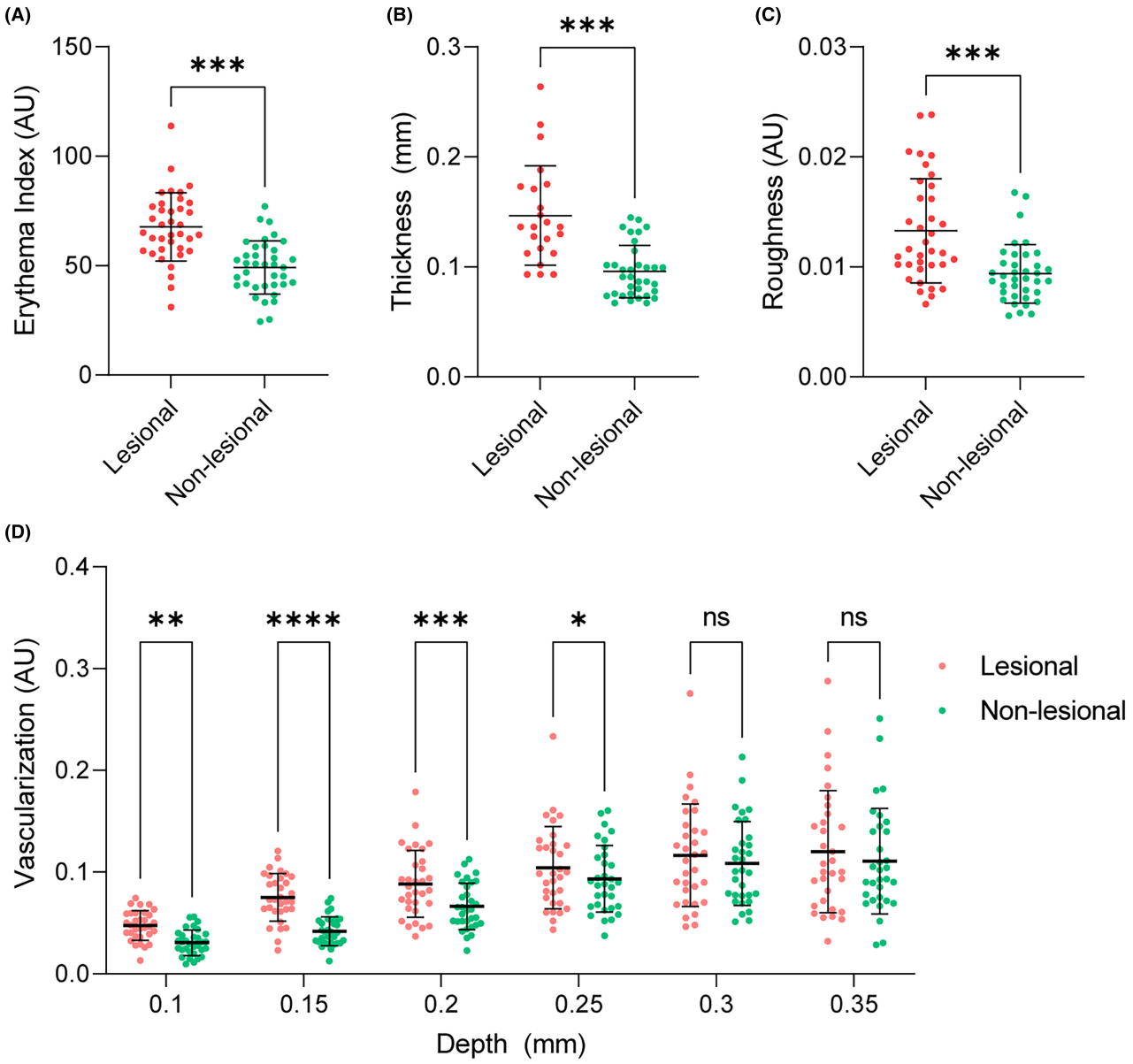

FIGURE 1 Erythema index as determined by standardized photography (A) and the epidermal thickness (B), superficial roughness (C) and the degree of vascularization at different depths in the epidermis (D) as determined by optical coherence tomography of lesional and non-lesional skin. Epidermal thickness could only be determined in 23 of 37 lesional and 34 of 37 non-lesional measurements. AU, arbitrary units; NS, not significant.

$p > 0.23$, for bacteria and fungi respectively, Figure 2A,C), indicating biodiversity on average did not differ between skin sites. However, *Staphylococcus* was significantly overrepresented and *Cutibacterium* significantly underrepresented in lesional skin compared to non-lesional skin (44.05% vs. 19.50% and 23.04% vs. 38.20%, respectively, $p \leq 0.001$, Figure 2B). The mycobiome proved small with only three genera present over the detection thresholds used (Figure 2D), of which over 80% comprised of *Malassezia* hits in both lesional and non-lesional skin without any significant differences (82.20% vs. 83,52%, $p > 0.05$). Due to the limitations associated with reliable identification of *Malassezia* at the species-level using ITS-sequencing, axenic culture plates were taken and subsequent MALDI-TOF MS was performed as a more specific qualitative alternative. Using *Malassezia* specific protocols successful isolation and identification of 16 from 37 lesional and 18 from 37 non-lesional samples was possible. No clear differences were observed between skin sites with *M. sympodialis* being the most prevalent at both sites (21.6% and 18.9% on lesional and non-lesional skin, respectively), followed by *M. slooffiae* (13.5%) on lesional and *M. globosa* (13.5%) on non-lesional skin (Figure 2E).

3.3 | Skin barrier

Finally, the skin barrier was studied as it represents the interface between external pathogens and the established epidermal inflammation. TEWL was used as an endpoint for skin barrier integrity and was significantly higher in lesional skin compared to non-lesional skin indicating an impaired barrier function (35.89 g/m^2/h vs. 21.27 g/m^2/h, $p > 0.001$, Figure 3A). Sebum levels were not significantly different between lesional and non-lesional skin (90.70 ± 54.93 vs. 82.78 ± 53.29, $p = 0.521$, Figure S4). The relative abundance was determined of all 12 major ceramide classes. The lesional ceramide profile showed a significant increase in Cer[NS] and Cer[AS] (17.25% vs. 11.86% and 16.99% vs. 10.61%, respectively, $p \leq 0.001$) and significantly decreased abundance of Cer[NdS], Cer[EOS] (7.15% vs. 8.06% and 2.52% vs. 3.51%, respectively, $p \leq 0.01$) and Cer[NP], Cer[NH], Cer[AP] (10.58% vs. 14.29%, 10.87% vs. 12.23%, 13.22% vs. 16.03%, respectively, $p \leq 0.001$, Figure 3B) compared to non-lesional skin. The abundance of other classes was not significantly different. The skewing of ceramide subclass synthesis can be easily interpreted by comparing the abundance of Cer[NS] and Cer[NP]. Indeed, alterations in lipid processing were evident from a significant increase of the Cer[NS]:Cer[NP] ratio in lesional compared to non-lesional skin (1.68 vs. 0.87, $p \leq 0.001$, Figure 3C). Additionally, the presence of Cer[NSc34], a Cer[NS] species with a total chain length of 34 carbons, was significantly elevated in lesional compared to non-lesional skin (8.19% vs. 5.10%, $p \leq 0.001$, Figure 3D). Using the monounsaturation in Cer[NS] as an indicator for the overall monounsaturation, ceramides at lesional skin sites were further impacted by a higher degree of unsaturation compared to non-lesional skin (7.32% vs. 3.71%, $p \leq 0.001$, Figure 3E). Lastly, lipid elongation was impaired in lesional skin as evident from a decreased average total carbon chain length of the ceramides compared to non-lesional skin (42.64 carbons vs. 43.85 carbons, $p \leq 0.001$, Figure 3F).

Visualization of the roughly 300 individual ceramide responses using dimension reduction analysis by PCA showed two distinguishable populations when stratifying for skin site (Figure 3G). This indicates the ceramide profile of lesional skin is alike between subjects, but differs from non-lesional skin. Plotting the TEWL values against ceramide parameters revealed a positive correlation for ceramide Cer[NS]:Cer[NP] ratio ($r = 0.6474$), amount of Cer[NSc34] ($r = 0.5170$) and degree of unsaturation ($r = 0.5920$) and a negative correlation against the ceramide chain length ($r = -0.6668$) (Figure 3H–K).

3.4 | Integration of results

Integration of quantitative clinical characteristics (Figure 1A,C,D), microbial properties (Figure 2A–D) and barrier parameters (Figure 3A–F) was performed using the entire dataset. The resulting PCA shows two distinguishable sets of data points with minimal overlap when stratifying for site (Figure 4A). The abundance of Cer[NS], the carbon chain length and the Cer[NS]:Cer[NP] ratio contribute most to the overall differential analysis (Table S4). Min-max normalized visualization of the most significant findings in a radar chart underline that the biggest differences are observed in the barrier compartment followed by inflammation (Figure 4B). Small differences between lesional and non-lesional skin were observed in the microbial parameters, with only the abundance of *Staphylococcus* being markedly different.

4 | DISCUSSION

SD is a multifactorial disease in which the interplay between the cutaneous microbiome, especially the presence of *Malassezia*, impaired skin barrier function and abnormal immunological responses seem integral to its pathogenesis.[1] In this study we comprehensively and non-invasively characterized the clinical representation of mild-to-moderate SD. We demonstrated a profound involvement of cutaneous barrier dysfunction with only small alterations in the microbiome, including the abundance of *Malassezia*, based on differences between lesional and non-lesional skin. This trial was performed in a sizeable number of 37 patients with similar disease burden after appropriate wash-outs and screening.

4.1 | Inflammation objectively quantified by OCT and standardized imaging

Visual assessment of SD, which includes the evaluation of erythema, is frequently used in daily clinical practice for disease monitoring. However, visual examination of the skin can be hampered by limited sensitivity, observer bias and overall intra- and inter-rater variability.[23,24] Therefore, we selected an objective approach to quantify

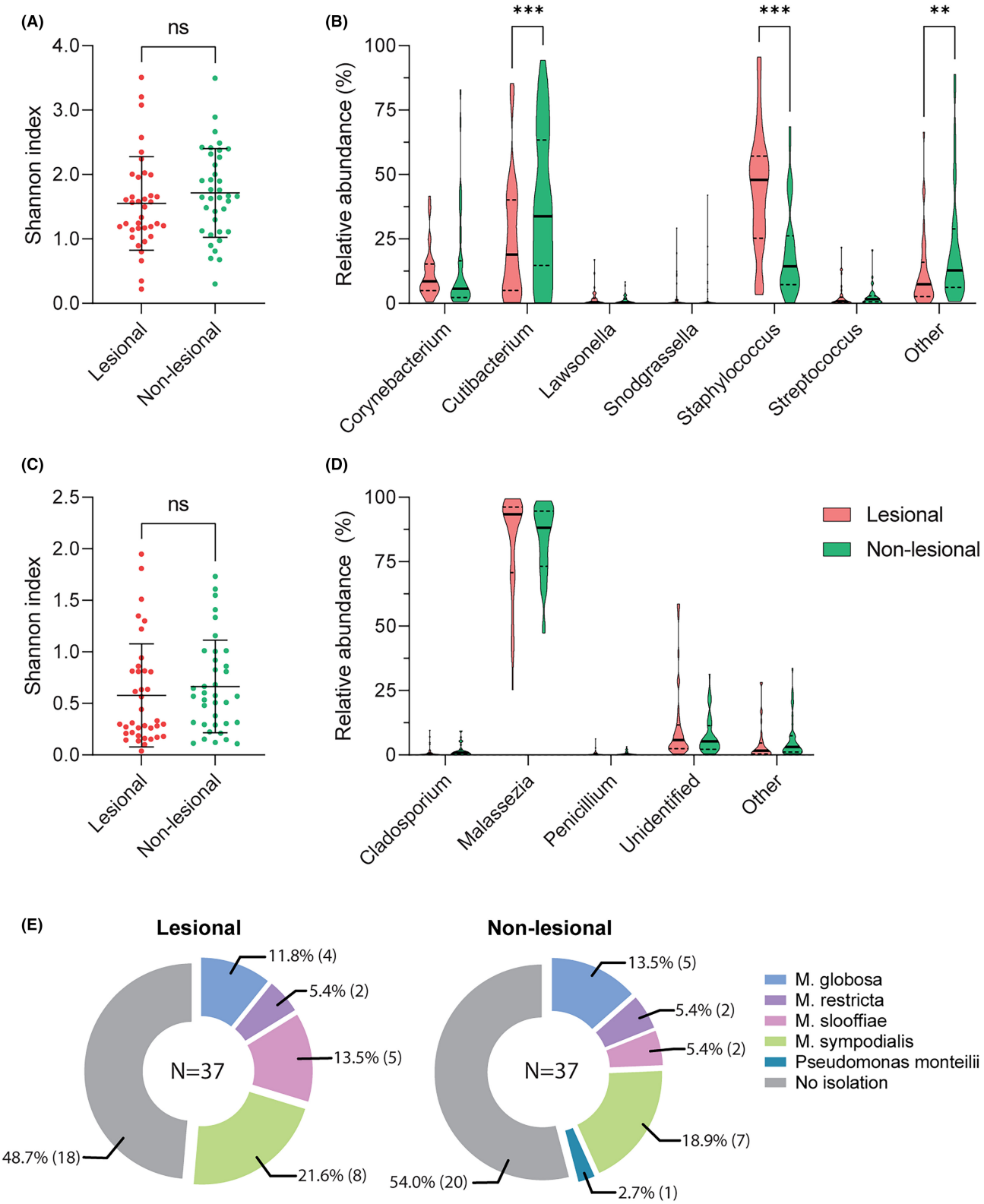

FIGURE 2 Bacterial Shannon diversity index (A) and composition of the bacterial microbiome (B) by 16s rRNA sequencing along with the fungal Shannon diversity index (C) and composition of the fungal microbiome (D) by ITS sequencing. The presented genera are filtered for minimal prevalence of 1% over all samples and presented relative to the total amount of microbes detected per analysis. Presence of different *Malassezia* species per site after isolation with contact plates and subsequent MALDI-TOF analysis (E). None of the samples yielded two or more different isolates.

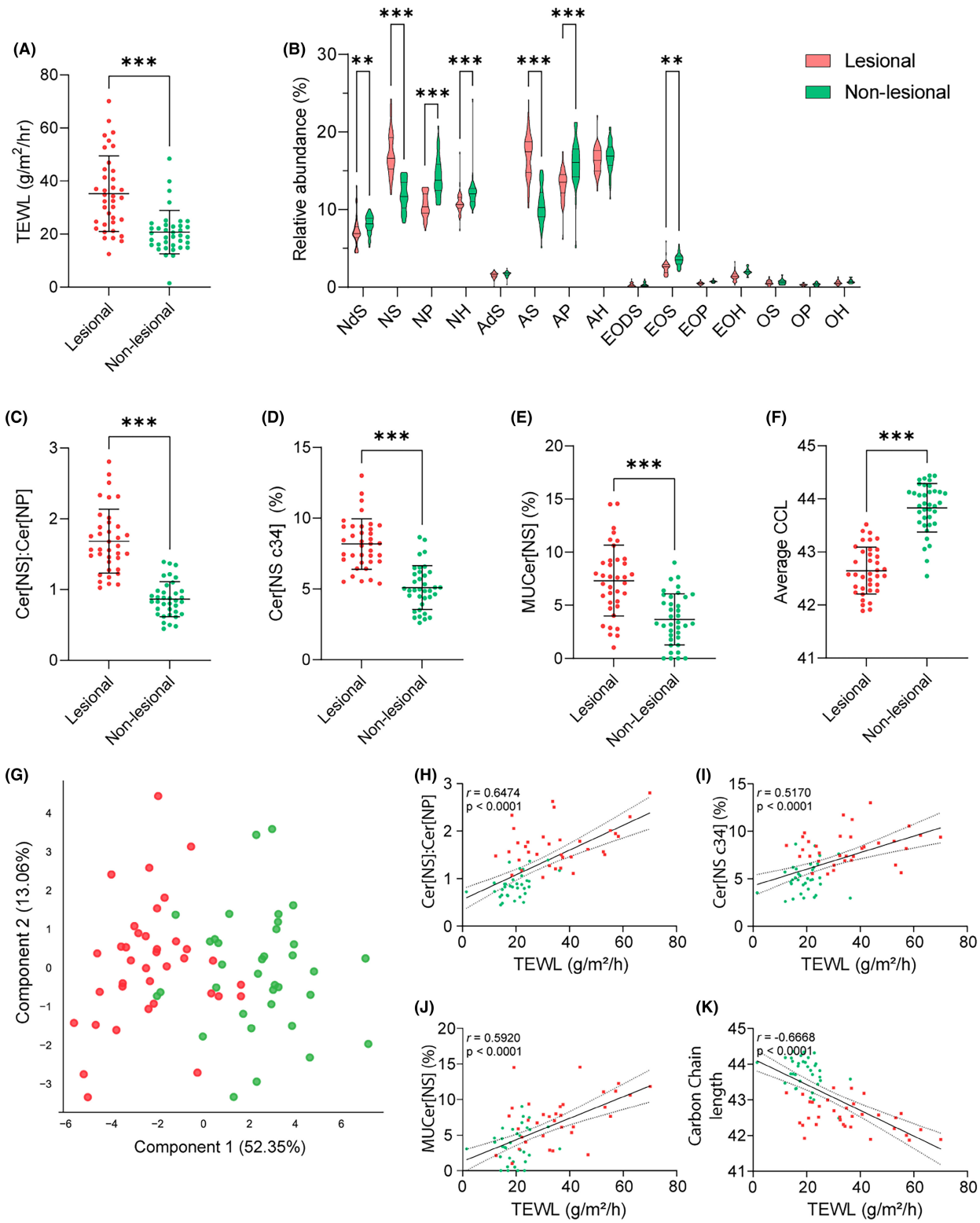

FIGURE 3 Barrier parameters of lesional compared to non-lesional skin demonstrate impaired barrier function in lesional skin. Functional barrier integrity is measured by trans-epidermal water loss (A). The ceramide profile is depicted after grouping individual ceramides per subclass (B), with the ratio between the abundance of Cer[NS] and Cer[NP] highlighted (C). The abundance of short ceramide species Cer[NSc34] (D) and degree of unsaturation (E) within Cer[NS] is shown. The average carbon chain length (CCL) of the combined sphingosine base and fatty acid tail within the non-Cer[EO] moiety is depicted (F). PCA analysis using all individual detected saturated ceramides yields two distinct population (G). Axes list the percentage of variance explained by the first two principal components, with the proximity of datapoints indicating similarity between samples. Correlations between TEWL and Cer[NS]:Cer[NP] (H), percentage Cer[NSc34] (I), percentage of unsaturation (J) and CCL (K) are shown with a line representing the optimal fit from linear regression analysis and 95% confident interval and Pearson's correlation coefficient. CCL, carbon chain length; MUCer, monounsaturated ceramide; TEWL, Trans-Epidermal Water Loss.

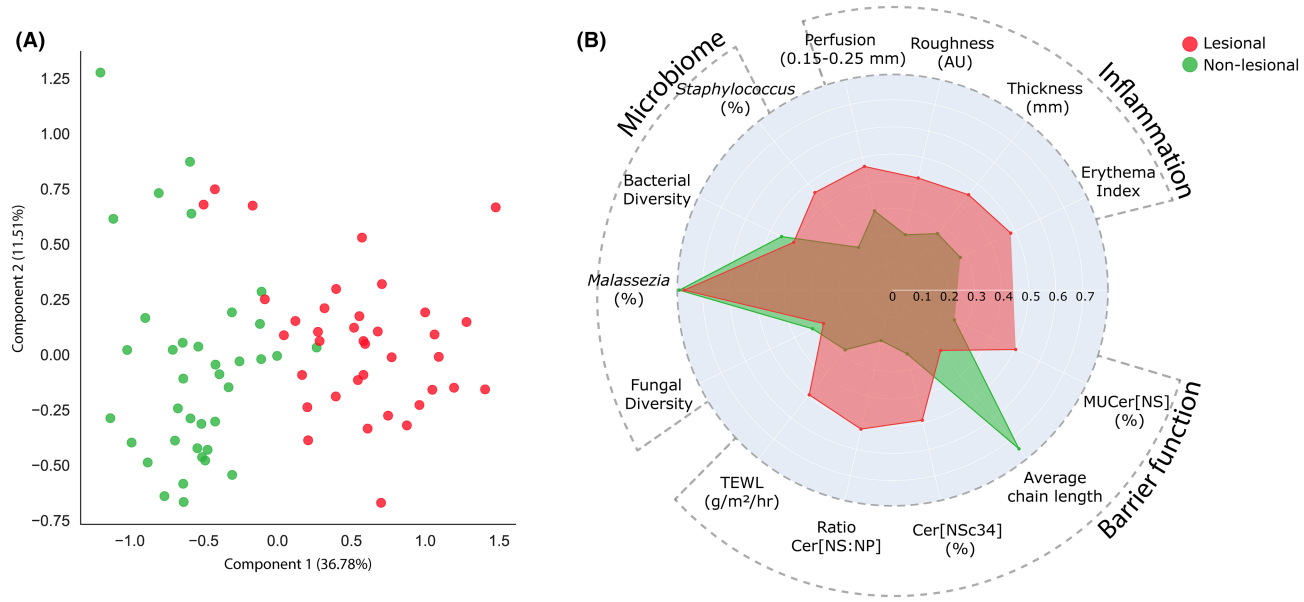

FIGURE 4 Principal component analysis (PCA) of lesional and non-lesional skin using all individual datapoints (A). Axes list the percentage of variance explained by the first two principal components. Integrative visualization of major contributors within the three different axes by radar chart (B). The distance of a datapoint from the center represent the average value per parameter per site compared to the average value per parameter of both sites. AU, arbitrary units; CCL, carbon chain length; MUCer, monounsaturated ceramide; TEWL, Trans-Epidermal Water Loss.

cutaneous inflammation. Digitalized erythema assessments have been reported but not applied to SD.[25–28] Here, standardized cross-polarized light photography is used to capture consistent images and enhanced erythema,[29] resulting in a clear differentiation between lesional and non-lesional skin. Optical biopsies by OCT enabled the determination of additional (sub)cutaneous parameters. Inflammatory characteristics such as increased perfusion[30] and epidermal thickness, corresponding to acanthosis,[31,32] were observed in lesional skin. Furthermore, a rougher lesional skin surface corresponds to the scaly phenotype of the disease.[1] Increased blood flow and epidermal thickness have been observed by OCT in the involved skin of psoriasis and atopic dermatitis patients compared to uninvolved skin and healthy controls.[33,34] Stand-alone, but also combined, standardized photography and OCT qualify as valuable non-invasive tools which enable sensitive and selective endpoints for disease monitoring and detection of treatment responses in clinical trials.[35]

4.2 | *Malassezia* and *Staphylococcus* dominate the lesional microbiome

Bacterial analysis of the skin surface showed an increased abundance of *Staphylococcus* and decreased abundance of *Cutibacterium* on lesional skin which concurs with previous SD profiling studies.[14,36] *Staphylococcus*, and especially *S. aureus*, is considered to be a pro-inflammatory mediator in atopic dermatitis.[37] While limited phylogenetic resolution prevents the identification of *S. aureus* in this study, the observed increase of *Staphylococcus* combined with reports that *S. aureus* is more abundant in SD patients compared to healthy controls might indicate bacterial involvement in SD pathogenesis.[38] Despite reports of bacterial involvement in SD, microbial involvement remains primarily focussed on *Malassezia* as a key pathogen. However, no differences were observed between the abundance of *Malassezia* on lesional and non-lesional skin. This is in accordance with findings showing the presence of *Malassezia* is neither limited to lesional skin nor SD patients.[3,6,14] Additionally, facial skin of healthy volunteers also showed a seemingly small and *Malassezia* dominated mycobiome.[39,40] Although it is hypothesised that specific *Malassezia* species might be responsible for instigating inflammation as virulence factors differ between *Malassezia* species,[41–43] no significant differences on species level were observed in this study. Culturing led to successful isolation of *Malassezia* species in approximately half of the subjects, illustrating the known challenges of isolating *Malassezia* from clinical samples.[44] Except for *M. slooffiae*, all species are relatively frequently isolated from healthy and SD skin.[45] Remarkably, *M. slooffiae* has been reported to have little virulence when directly compared to *M. globosa* and *M. sympodialis*.[42] However, intra-species variation in virulence has been reported indicating that microbial activity rather than abundance is an important factor for the association of specific species to lesional skin.[46,47] Based on these results, it seems too straightforward to attribute SD pathogenesis to the presence of *Malassezia* alone.

4.3 | Substantial functional and compositional barrier alterations

Until now, the limited studies that have demonstrated functional barrier impairment in SD have neglected the lipid compartment

as barrier component.[48,49] In this study, we show a substantially impacted barrier in lesional skin on functional grounds by TEWL and demonstrate concomitant changes in the ceramide profile. These compositional changes correlated with the degree of barrier impairment as judged by TEWL. In line with our study in SD, changes in the Cer[NS]:Cer[NP] ratio,[50] degree of unsaturation,[51] ceramide chain length[12,52] and presence of extremely short chain Cer[NSc34][12,51,53,54] in lesional skin have been observed in atopic dermatitis where barrier involvement is firmly established. These changes to the lipid profile appear to be induced by inflammation as lipid alterations can be evoked by atopic dermatitis and psoriasis associated pro-inflammatory cytokines *in vitro*[55–57] and normalize in response to anti-inflammatory treatment in atopic dermatitis patients.[52] Whether these alterations are therefore primarily linked to inflammation and only coincide with barrier dysfunction has been investigated in mechanistic studies using lipid model systems. Lacking an inflammatory component, these models have shown that increased Cer[NS],[58,59] increased unsaturation[60] and decreased lipid chain length[61] directly increase permeability. Additionally, studies in healthy volunteers have shown Cer[NS]:Cer[NP] ratios in the face comparable to non-lesional skin without a location-dependent effect on Cer[NSc34] abundances.[62,63] It is of note that total ceramide levels can change with age and seasons as demonstrated in healthy skin and acne, but without much effect on the relative ceramide subclass composition as reported on in the current study.[62,64,65] Additionally, the impact of these factors might be limited as patients serve as their own control. The predilection of SD lesions with areas known for increased water loss such as the mouth, eyelids and nasolabial folds might be confounding for the increased TEWL.[49,66] Indeed, healthy volunteers have shown TEWL values at the nasolabial fold that approach the lesional values observed in this study with comparable TEWL values at the cheek or forehead, sites where non-lesional measurements were often conducted.[67,68] Therefore, increased TEWL values in lesional skin may not reflect barrier impairment but rather indicate differences in normal physiological functioning between skin sites. However, the concurrent correlations between the TEWL values and ceramide composition reaffirm the interdependence of SD functional barrier impairment and ceramide-compositional alterations.

4.4 | Integrative data analysis emphasizes importance of barrier dysfunction

An integrative approach was taken to visualize the data after investigating the three hallmarks of SD separately. Using PCA, we elucidated which parameters of our dataset predominantly contribute to the SD phenotype. The abundance of Cer[NS] and ceramide chain length showed to be the most important discriminating features. Indeed, the radar plot directs emphasis towards barrier function with little differences in the micro- and mycobiome. While the contribution of *Malassezia* seems to be negligible when only considering relative abundances, it should be re-emphasized that SD appears to be neither caused solely by barrier dysfunction nor microbial involvement but rather by the interplay between factors. This finding correlates with the shifting belief in literature that *Malassezia* might not be solely responsible for causing SD.[5,6] This highlights the added value of a multimodal and integrative approach to disease profiling which enables in-depth characterization with the possibility to unravel part of pathogenesis.[35]

5 | CONCLUSION

In conclusion, this study demonstrates the importance of the barrier-inflammation axis in mild-to-moderate SD which seems to be more prominently involved compared to the microbiome. While not incorporating an internal healthy control group, our results are compared thoroughly with prior research in healthy volunteers through literature. Moreover, the results agree with and support existing literature regarding inflammation and microbial involvement in SD while complementing the current understanding of barrier dysfunction in SD. Barrier impairment parallels that of atopic dermatitis where emollients are used effectively.[69] Treating SD by improving the skin barrier function has been proposed as a potential adjuvant therapy,[70] but the management of SD remains focussed on anti-inflammatory and anti-fungal treatments.[71] Taken together, the incorporation of emollients, humectants or other barrier repair agents should not be neglected in the management of SD and might support current treatment modalities.

AUTHOR CONTRIBUTIONS

Robert Rissmann, Joke A. Bouwstra, Martijn B.A. van Doorn, Tessa Niemeyer-van der Kolk, Gary L. Feiss, Rob J. Vreeken designed the research study. Jannik Rousel, Andreea Nădăban, Mahdi Saghari, Lisa Pagan, Bart Theelen, Tom Gambrah, Tessa Niemeyer-van der Kolk and Martijn B.A. van Doorn performed the research under supervision of Robert Rissmann, Martijn B.A. van Doorn and Jacobus Burggraaf. Jannik Rousel, Bart Theelen, Hein E.C. van der Wall, Ahnjili Zhuparris analysed the data. Jannik Rousel, Martijn B.A. van Doorn, Jacobus Burggraaf and Robert Rissmann wrote the first manuscript draft. All authors have read and approved the final manuscript.

ACKNOWLEDGMENTS

The authors are grateful to all participating patients and the clinical network for trials in dermatology, CONNECTED, for the support.

FUNDING INFORMATION

The study was sponsored by Cutanea Life Sciences, Wayne, Pennsylvania, USA and Maruho Co. Ltd., Kyoto, Japan. The sponsors had no role in study conduct, data analysis or the interpretation of the data.

CONFLICT OF INTEREST STATEMENT

GF was an employee of Cutanea Life Sciences who funded the study and was involved in the study design and review and approval of the

final manuscript. The other authors have no conflicts of interest to declare.

DATA AVAILABILITY STATEMENT

The data supporting the figures and tables in this article are available upon request.

ORCID

Jannik Rousel https://orcid.org/0000-0003-0986-3753
Andreea Năděban https://orcid.org/0000-0002-4981-6268
Mahdi Saghari https://orcid.org/0000-0002-3829-0037
Lisa Pagan https://orcid.org/0000-0002-2064-7501
Bart Theelen https://orcid.org/0000-0003-1333-2058
Jacobus Burggraaf https://orcid.org/0000-0001-7912-0918

REFERENCES

1. Borda LJ, Wikramanayake TC. Seborrheic dermatitis and dandruff: a comprehensive review. *J Clin Investig Dermatol*. 2015;3(2). doi:10.13188/2373-1044.1000019
2. Goldenberg G. Optimizing treatment approaches in seborrheic dermatitis. *J Clin Aesthet Dermatol*. 2013;6(2):44.
3. del Rosso JQ, Kim GK. Seborrheic dermatitis and Malassezia species: how are they related? *J Clin Aesthet Dermatol*. 2009;2(11):14.
4. Juntachai W, Oura T, Murayama SY, Kajiwara S. The lipolytic enzymes activities of Malassezia species. *Med Mycol*. 2009;47(5):477-484. doi:10.1080/13693780802314825
5. Adalsteinsson JA, Kaushik S, Muzumdar S, Guttman E, Ungar J. An update on the microbiology, immunology and genetics of seborrheic dermatitis. *Exp Dermatol*. 2020;29(5):481-489. doi:10.1111/EXD.14091
6. Wikramanayake TC, Borda LJ, Miteva M, Paus R. Seborrheic dermatitis—looking beyond Malassezia. *Exp Dermatol*. 2019;28(9):991-1001. doi:10.1111/EXD.14006
7. Goh JPZ, Ruchti F, Poh SE, et al. The human pathobiont Malassezia furfur secreted protease Mfsap1 regulates cell dispersal and exacerbates skin inflammation. *Proc Natl Acad Sci*. 2022;119(49):e2212533119. doi:10.1073/PNAS.2212533119
8. Proksch E, Brandner JM, Jensen JM. The skin: an indispensable barrier. *Exp Dermatol*. 2008;17(12):1063-1072. doi:10.1111/J.1600-0625.2008.00786.X
9. Uche LE, Gooris GS, Bouwstra JA, Beddoes CM. High concentration of the ester-linked ω-hydroxy ceramide increases the permeability in skin lipid model membranes. *Biochimica et Biophysica acta (BBA) Biomembr*. 2021;1863(1):183487. doi:10.1016/J.BBAMEM.2020.183487
10. Beddoes CM, Gooris GS, Barlow DJ, et al. The importance of ceramide headgroup for lipid localisation in skin lipid models. *Biochim Biophys Acta Biomembr*. 2022;1864(6):183886. doi:10.1016/J.BBAMEM.2022.183886
11. Ishikawa J, Narita H, Kondo N, et al. Changes in the ceramide profile of atopic dermatitis patients. *J Invest Dermatol*. 2010;130(10):2511-2514. doi:10.1038/JID.2010.161
12. Janssens M, van Smeden J, Gooris GS, et al. Increase in short-chain ceramides correlates with an altered lipid organization and decreased barrier function in atopic eczema patients. *J Lipid Res*. 2012;53(12):2755-2766. doi:10.1194/JLR.P030338
13. Elias PM. Optimizing emollient therapy for skin barrier repair in atopic dermatitis. *Ann Allergy Asthma Immunol*. 2022;128(5):505-511. doi:10.1016/J.ANAI.2022.01.012
14. Tao R, Li R, Wang R. Skin microbiome alterations in seborrheic dermatitis and dandruff: a systematic review. *Exp Dermatol*. 2021;30(10):1546-1553. doi:10.1111/EXD.14450
15. Baysal V, Yildirim M, Ozcanli C, Ceyhan AM. Itraconazole in the treatment of seborrheic dermatitis: a new treatment modality. *Int J Dermatol*. 2004;43(1):63-66. doi:10.1111/J.1365-4632.2004.02123.X
16. Elman S, Hynan LS, Gabriel V, Mayo MJ. The 5-D itch scale: a new measure of pruritus. *Br J Dermatol*. 2010;162(3):587-593. doi:10.1111/J.1365-2133.2009.09586.X
17. Finlay AY, Khan GK. Dermatology life quality index (DLQI)—a simple practical measure for routine clinical use. *Clin Exp Dermatol*. 1994;19(3):210-216. doi:10.1111/j.1365-2230.1994.tb01167.x
18. Basra MKA, Fenech R, Gatt RM, Salek MS, Finlay AY. The Dermatology Life Quality Index 1994–2007: a comprehensive review of validation data and clinical results. *Br J Dermatol*. 2008;159(5):997-1035. doi:10.1111/J.1365-2133.2008.08832.X
19. Yamamoto T, Takiwaki H, Arase S, Ohshima H. Derivation and clinical application of special imaging by means of digital cameras and image J freeware for quantification of erythema and pigmentation. *Skin Res Technol*. 2008;14(1):26-34. doi:10.1111/J.1600-0846.2007.00256.X
20. Kolecka A, Khayhan K, Arabatzis M, et al. Efficient identification of Malassezia yeasts by matrix-assisted laser desorption ionization-time of flight mass spectrometry (MALDI-TOF MS). *Br J Dermatol*. 2014;170(2):332-341. doi:10.1111/BJD.12680
21. Boiten W, Absalah S, Vreeken R, Bouwstra J, van Smeden J. Quantitative analysis of ceramides using a novel lipidomics approach with three dimensional response modelling. *Biochim Biophys Acta*. 2016;1861(11):1652-1661. doi:10.1016/J.BBALIP.2016.07.004
22. Motta S, Monti M, Sesana S, Caputo R, Carelli S, Ghidoni R. Ceramide composition of the psoriatic scale. *Biochim Biophys Acta*. 1993;1182(2):147-151. doi:10.1016/0925-4439(93)90135-N
23. Poon TSC, Kuchel JM, Badruddin A, et al. Objective measurement of minimal erythema and melanogenic doses using natural and solar-simulated light. *Photochem Photobiol*. 2003;78(4):331-336. doi:10.1562/0031-8655(2003)0780331OMOMEA2.0.CO2
24. Ten Voorde W, Saghari M, Boltjes J, et al. A multimodal, comprehensive characterization of a cutaneous wound model in healthy volunteers. *Exp Dermatol*. 2023;00:1-14. doi:10.1111/EXD.14808
25. Logger JGM, de Jong EMGJ, Driessen RJB, van Erp PEJ. Evaluation of a simple image-based tool to quantify facial erythema in rosacea during treatment. *Skin Res Technol*. 2020;26(6):804-812. doi:10.1111/SRT.12878
26. Ohshima H, Takiwaki H, Washizaki K, Ishiko A, Itoh M, Kanto H. Quantitative evaluation of patch test reactions: a comparison between visual grading and erythema index image analysis. *Skin Res Technol*. 2011;17(2):220-225. doi:10.1111/J.1600-0846.2010.00488.X
27. Tao M, Li M, Zhang Y, et al. Objectively quantifying facial erythema in rosacea aided by the ImageJ analysis of VISIA red images. *Skin Res Technol*. 2023;29(1):e13241. doi:10.1111/SRT.13241
28. Frew J, Penzi L, Suarez-Farinas M, et al. The erythema Q-score, an imaging biomarker for redness in skin inflammation. *Exp Dermatol*. 2021;30(3):377-383. doi:10.1111/EXD.14224
29. Oh Y, Markova A, Noor SJ, Rotemberg V. Standardized clinical photography considerations in patients across skin tones. *Br J Dermatol*. 2022;186(2):352-354. doi:10.1111/BJD.20766
30. Rajabi-Estarabadi A, Tsang DC, Nouri K, Tosti A. Evaluation of positive patch test reactions using optical coherence tomography: a pilot study. *Skin Res Technol*. 2019;25(5):625-630. doi:10.1111/SRT.12695
31. Odorici G, Losi A, Ciardo S, Pellacani G, Conti A. Non-invasive evaluation of Secukinumab efficacy in severe plaque psoriasis with confocal microscopy and optical coherence tomography: a case report. *Skin Res Technol*. 2018;24(1):160-162. doi:10.1111/SRT.12409

32. Yélamos O, Alejo B, Ertekin SS, et al. Non-invasive clinical and microscopic evaluation of the response to treatment with clobetasol cream vs. calcipotriol/betamethasone dipropionate foam in mild to moderate plaque psoriasis: an investigator-initiated, phase IV, unicentric, open, randomized clinical trial. *J Eur Acad Dermatol Venereol*. 2021;35(1):143-149. doi:10.1111/JDV.16559
33. Byers RA, Maiti R, Danby SG, et al. Sub-clinical assessment of atopic dermatitis severity using angiographic optical coherence tomography. *Biomed Opt Express*. 2018;9(4):2001-2017. doi:10.1364/BOE.9.002001
34. Ha-Wissel L, Yasak H, Huber R, et al. Case report: optical coherence tomography for monitoring biologic therapy in psoriasis and atopic dermatitis. *Front Med (Lausanne)*. 2022;9:2932. doi:10.3389/FMED.2022.995883/BIBTEX
35. Rissmann R, Moerland M, van Doorn MBA. Blueprint for mechanistic, data-rich early phase clinical pharmacology studies in dermatology. *Br J Clin Pharmacol*. 2020;86(6):1011-1014. doi:10.1111/BCP.14293
36. Sanders MGH, Nijsten T, Verlouw J, Kraaij R, Pardo LM. Composition of cutaneous bacterial microbiome in seborrheic dermatitis patients: a cross-sectional study. *PloS One*. 2021;16(5):e0251136. doi:10.1371/JOURNAL.PONE.0251136
37. Geoghegan JA, Irvine AD, Foster TJ. Staphylococcus aureus and atopic dermatitis: a complex and evolving relationship. *Trends Microbiol*. 2018;26(6):484-497. doi:10.1016/J.TIM.2017.11.008
38. Tamer F, Yuksel M, Sarifakioglu E, Karabag Y. Staphylococcus aureus is the most common bacterial agent of the skin flora of patients with seborrheic dermatitis. *Dermatol Pract Concept*. 2018;8(2):80-84. doi:10.5826/DPC.0802A04
39. Findley K, Oh J, Yang J, et al. Topographic diversity of fungal and bacterial communities in human skin. *Nature*. 2013;498(7454):367-370. doi:10.1038/nature12171
40. Tao R, Li R, Wang R, Tao R, Li R, Wang R. Comparative analysis of the facial microbiome between rosacea and seborrheic dermatitis. *Indian J Dermatol Venereol Leprol*. 2023;1:1-3. doi:10.25259/IJDVL_215_2022
41. Grice EA, Dawson TL. Host–microbe interactions: Malassezia and human skin. *Curr Opin Microbiol*. 2017;40:81-87. doi:10.1016/J.MIB.2017.10.024
42. Angiolella L, Rojas F, Mussin J, et al. Biofilm formation, adherence, and hydrophobicity of M. Sympodialis, M. Globosa, and M. Slooffiae from clinical isolates and normal skin virulence factors of M. Sympodialis, M. Globosa and M. Slooffiae. *Med Mycol*. 2020;58(8):1162-1168. doi:10.1093/MMY/MYAA017
43. Theelen B, Cafarchia C, Gaitanis G, Bassukas ID, Boekhout T, Dawson TL. Malassezia ecology, pathophysiology, and treatment. *Med Mycol*. 2018;56(suppl_1):S10-S25. doi:10.1093/MMY/MYX134
44. Abdillah A, Ranque S. MalaSelect: a selective culture medium for Malassezia species. *J Fungi*. 2021;7(10):824. doi:10.3390/JOF7100824
45. Prohic A, Jovovic Sadikovic T, Krupalija-Fazlic M, Kuskunovic-Vlahovljak S. Malassezia species in healthy skin and in dermatological conditions. *Int J Dermatol*. 2016;55(5):494-504. doi:10.1111/IJD.13116
46. Angiolella L, Leone C, Rojas F, Mussin J, de Los Angeles Sosa M, Giusiano G. Biofilm, adherence, and hydrophobicity as virulence factors in Malassezia furfur. *Med Mycol*. 2018;56(1):110-116. doi:10.1093/MMY/MYX014
47. Chebil W, Rhimi W, Haouas N, et al. Virulence factors of Malassezia strains isolated from pityriasis versicolor patients and healthy individuals. *Med Mycol*. 2022;60(8):60. doi:10.1093/MMY/MYAC060
48. Tollesson A, Frithz A. Transepidermal water loss and water content in the stratum corneum in infantile seborrhoeic dermatitis. *Acta Derm Venereol*. 1993;73(1):18-20. doi:10.2340/00015555731820
49. Suchonwanit P, Triyangkulsri K, Ploydaeng M, Leerunyakul K. Assessing biophysical and physiological profiles of scalp seborrheic dermatitis in the Thai population. *Biomed Res Int*. 2019;2019:1-6. doi:10.1155/2019/5128376
50. Yokose U, Ishikawa J, Morokuma Y, et al. The ceramide [NP]/[NS] ratio in the stratum corneum is a potential marker for skin properties and epidermal differentiation. *BMC Dermatol*. 2020;20(1):6. doi:10.1186/S12895-020-00102-1
51. Danso M, Boiten W, van Drongelen V, et al. Altered expression of epidermal lipid bio-synthesis enzymes in atopic dermatitis skin is accompanied by changes in stratum corneum lipid composition. *J Dermatol Sci*. 2017;88(1):57-66. doi:10.1016/J.JDERMSCI.2017.05.005
52. Berdyshev E, Goleva E, Bissonnette R, et al. Dupilumab significantly improves skin barrier function in patients with moderate-to-severe atopic dermatitis. *Allergy*. 2022;77(11):3388-3397. doi:10.1111/ALL.15432
53. Ito S, Ishikawa J, Naoe A, et al. Ceramide synthase 4 is highly expressed in involved skin of patients with atopic dermatitis. *J Eur Acad Dermatol Venereol*. 2017;31(1):135-141. doi:10.1111/JDV.13777
54. Kim BK, Shon JC, Seo HS, et al. Decrease of ceramides with long-chain fatty acids in psoriasis: possible inhibitory effect of interferon gamma on chain elongation. *Exp Dermatol*. 2022;31(2):122-132. doi:10.1111/EXD.14431
55. Danso MO, van Drongelen V, Mulder A, et al. TNF-α and Th2 cytokines induce atopic dermatitis-like features on epidermal differentiation proteins and stratum corneum lipids in human skin equivalents. *J Invest Dermatol*. 2014;134(7):1941-1950. doi:10.1038/JID.2014.83
56. Tawada C, Kanoh H, Nakamura M, et al. Interferon-γ decreases ceramides with long-chain fatty acids: possible involvement in atopic dermatitis and psoriasis. *J Invest Dermatol*. 2014;134(3):712-718. doi:10.1038/JID.2013.364
57. Berdyshev E, Goleva E, Bronova I, et al. Lipid abnormalities in atopic skin are driven by type 2 cytokines. *JCI. Insight*. 2018;3(4):e98006. doi:10.1172/JCI.INSIGHT.98006
58. Uche LE, Gooris GS, Bouwstra JA, Beddoes CM. Barrier capability of skin lipid models: effect of ceramides and free fatty acid composition. *Langmuir*. 2019;35(47):15376-15388. doi:10.1021/ACS.LANGMUIR.9B03029
59. Nădăban A, Rousel J, El Yachioui D, et al. Effect of sphingosine and phytosphingosine ceramide ratio on lipid arrangement and barrier function in skin lipid models. *The Effect of Sphingosine and Phytosphingosine Ceramide Ratio on Lipid Arrangement and Barrier Functionality in Skin Lipid Models*. Published online; 2023.
60. Mojumdar EH, Helder RWJ, Gooris GS, Bouwstra JA. Monounsaturated fatty acids reduce the barrier of stratum corneum lipid membranes by enhancing the formation of a hexagonal lateral packing. *Langmuir*. 2014;30(22):6534-6543. doi:10.1021/LA500972W
61. Uche LE, Gooris GS, Bouwstra JA, Beddoes CM. Increased levels of short-chain ceramides modify the lipid organization and reduce the lipid barrier of skin model membranes. *Langmuir*. 2021;37(31):9478-9489. doi:10.1021/ACS.LANGMUIR.1C01295
62. Ishikawa J, Shimotoyodome Y, Ito S, et al. Variations in the ceramide profile in different seasons and regions of the body contribute to stratum corneum functions. *Arch Dermatol Res*. 2013;305(2):151-162. doi:10.1007/S00403-012-1286-5
63. Mori S, Shiraishi A, Epplen K, et al. Characterization of skin function associated with obesity and specific correlation to local/systemic parameters in American women. *Lipids Health Dis*. 2017;16(1):214. doi:10.1186/S12944-017-0608-1
64. Rogers J, Harding C, Mayo A, Banks J, Rawlings A. Stratum corneum lipids: the effect of ageing and the seasons. *Arch Dermatol Res*. 1996;288(12):765-770. doi:10.1007/BF02505294
65. Pappas A, Kendall AC, Brownbridge LC, Batchvarova N, Nicolaou A. Seasonal changes in epidermal ceramides are linked to impaired

barrier function in acne patients. *Exp Dermatol*. 2018;27(8):833-836. doi:10.1111/EXD.13499
66. Voegeli R, Gierschendorf J, Summers B, Rawlings A v. Facial skin mapping: from single point bio-instrumental evaluation to continuous visualization of skin hydration, barrier function, skin surface pH, and sebum in different ethnic skin types. *Int J Cosmet Sci*. 2019;41(5):411-424. doi:10.1111/ICS.12562
67. Kobayashi H, Tagami H. Distinct locational differences observable in biophysical functions of the facial skin: with special emphasis on the poor functional properties of the stratum corneum of the perioral region. *Int J Cosmet Sci*. 2004;26(2):91-101. doi:10.1111/J.0412-5463.2004.00208.X
68. Voegeli R, Rawlings AV, Seroul P, Summers B. A novel continuous colour mapping approach for visualization of facial skin hydration and transepidermal water loss for four ethnic groups. *Int J Cosmet Sci*. 2015;37(6):595-605. doi:10.1111/ICS.12265
69. van Zuuren EJ, Fedorowicz Z, Christensen R, Lavrijsen A, Arents BWM. Emollients and moisturisers for eczema. *Cochrane Database Syst Rev*. 2017;2017(2):CD012119. doi:10.1002/14651858.CD012119.PUB2
70. Mangion SE, Mackenzie L, Roberts MS, Holmes AM. Seborrheic dermatitis: topical therapeutics and formulation design. *Eur J Pharm Biopharm*. 2023;185:148-164. doi:10.1016/J.EJPB.2023.01.023
71. Desai S, McCormick E, Friedman A. An up-to-date approach to the Management of Seborrheic Dermatitis. *J Drugs Dermatol*. 2022;21(12):1373-1374. doi:10.36849/JDD.1022

SUPPORTING INFORMATION

Additional supporting information can be found online in the Supporting Information section at the end of this article.

Data S1. Extended material and methods.

How to cite this article: Rousel J, Nădăban A, Saghari M, et al. Lesional skin of seborrheic dermatitis patients is characterized by skin barrier dysfunction and correlating alterations in the stratum corneum ceramide composition. *Exp Dermatol*. 2023;00:1-12. doi:10.1111/exd.14952